J Mol Model (2010) 16:431–436
DOI 10.1007/s00894-009-0544-8

ORIGINAL PAPER

Mechanistic study of palladium-catalyzed telomerization of 1,3-butadiene with methanol

Chun-Fang Huo · Ralf Jackstell · Matthias Beller · Haijun Jiao

Received: 11 May 2009 / Accepted: 9 June 2009 / Published online: 23 July 2009

Abstract The Pd-catalyzed telomerization in the presence of phosphine and carbene ligands has been computed. It is shown that the C–C coupling of the less stable complex **A** with one *trans*- and one *cis*-butadiene in *syn* orientation forms the most stable intermediate **B** and is favorable both kinetically and thermodynamically. Protonation of **B** leads to equilibrium of the two most stable isomers of intermediate **C**. The overall regioselectivity is favored thermodynamically.

Keywords C–C coupling · DFT · Palladium · Regioselectivity

Introduction

The Pd-catalyzed telomerization of 1,3-butadiene with nucleophiles, which combines simple starting materials in 100 % atom efficiency to give functionalized 2,7-octadienes [1–5], has attracted significant interest in recent years and can be considered as a green process. Due to their availability and low prices, 1,3-butadiene and alcohols (especially methanol) have been mainly investigated (Scheme 1). In general, the reaction leads to a mixture of two regioisomers: **1** as the major product is a useful precursor for plasticizer alcohols, solvents, corrosion inhibitors and monomers for polymers [1]; and **2** as the by-product is also of some commercial interests.

In order to develop more general and industrially viable catalysts for telomerizations a detailed understanding of the reaction mechanism is desirable. In the past elegant studies have been performed by Jolly and co-workers [6]. Later on, Beller *et al*. [7] modified the "Jolly-mechanism" on the basis of experimental studies. As shown in Scheme 2, the first step is the coordination of two 1,3-butadienes with a LPd(0) complex to form **A**, and the second step is the oxidative C–C coupling with the formation of LPd(η^1,η^3-octadiendiyl) **B**. Then protonation of **B** by methanol at the C6 atom of the C8-chain to form $[LPd(\eta^2,\eta^3\text{–}C_8H_{13})]^+$ **C** takes place. The last step is the nucleophilic attack of methoxide to the allylic terminus (path A) in **C** to form the regioselective linear (**D**-*n*) or branched (**D**-*iso*) isomers, respectively. Although **A** is unknown yet, **B** and **C** were observed experimentally. In contrast to **B**, which was characterized by X-ray analysis, no direct information about the structure of **C** was known. In addition to the main regioisomers (**1** and **2**), the formation of 1,3,7-octatriene from the deprotonation of **C** at C4 carbon of the C8-chain and 4-vinylcyclohexene from Diels-Alder reaction has been observed, but their chemoselectivity is rather low (< 1% for L = IMes and 2 % for L = PPh_3).

In recent years it was demonstrated that Pd carbene complexes constitute more active and productive catalysts compared to the corresponding phosphine complexes [8–13]. However, no detailed mechanistic insight for applying these novel catalysts is known. Here, we report the first

Dedicated to Professor Dr. T. Clark on the occasion of his 60th birthday

Electronic supplementary material The online version of this article (doi:10.1007/s00894-009-0544-8) contains supplementary material, which is available to authorized users.

C.-F. Huo · H. Jiao
State Key Laboratory of Coal Conversion,
Institute of Coal Chemistry, Chinese Academy of Sciences,
Taiyuan 030001, People's Republic of China

R. Jackstell · M. Beller · H. Jiao (✉)
Leibniz-Institut für Katalyse e.V. an der Universität Rostock,
Albert-Einstein-Strasse 29a,
18059 Rostock, Germany
e-mail: haijun.jiao@catalysis.de

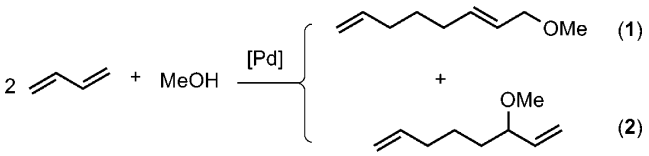

Scheme 1 Telomerization of 1,3-butadiene and methanol

theoretical elucidation and exploration of the reaction mechanism of the LPd(0)-catalyzed telomerization of 1,3-butadiene in the presence of carbene ligands. The entire catalytic cycle on the basis of Scheme 2 is explored at the B3LYP density functional level of theory (DFT). For direct comparison with the available experimental results [14–16], we have carried out computations on the real-sized Ph_3P and 1,3-dimesitylimidazol-2-ylidene carbene (IMes) systems.

Computational methods

All calculations were carried out by using the Gaussian 03 program [17]. All structures were first optimized at the B3LYP level of density functional theory with the LANL2DZ basis set [18, 19], and the nature of the optimized structures on the potential energy surface was characterized by the calculated number of imaginary frequency (NImag) at the same level of theory (B3LYP/LANL2DZ), *i.e.*, energy minimum structures without imaginary frequencies (NImag= 0), and transition states with only one imaginary frequency (NImag=1) [20], and the imaginary mode connects the reactant and product. The obtained structures were further refined at the B3LYP level with the LANL2DZ basis set including a set of polarization functions (LANL2DZ(d)) [18, 19]. These re-optimized structures are used for comparison. This method works well for Pd Chemistry [21]. For discussing the stability and reactivity we have used the relative Gibbs free energy (ΔG), which was computed at the B3LYP/LANL2DZ(d) level by taking the thermal correction to Gibbs free energy at 298 K from frequency calculations at the B3LYP/LANL2DZ level. The obtained free energy (ΔG) has been used to estimate the equilibrium of the related intermediates ($\Delta G = -RTlnK$). The computed energetic data and the optimized Cartesian coordinates for all isomers are given in the Supplementary material.

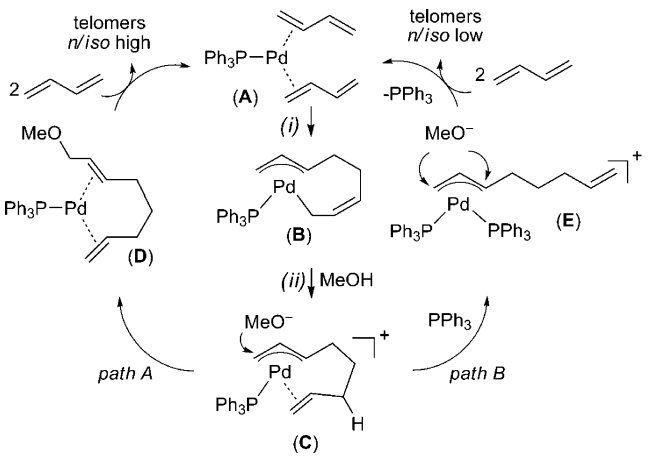

Scheme 2 Proposed telomerization mechanism of 1,3-butadiene and methanol

Results and discussion

Complex **A**

On the basis of the *trans* and *cis* isomers of 1,3-butadiene and their orientations in coordination with the LPd(0) complex, there are six isomers for complex **A** (Fig. 1). Here, *trans* and *cis* mean the conformation of *trans*- and *cis*-butadiene; and *anti* and *syn* show their relative orientation in **A**. It is to note that only LPd(0) complexes with butadiene in η^2-mode have been located, and attempts to get the η^4-mode failed. All six isomers are located as energy minimum structures on the potential energy surface. As expected, **A-2trans-anti** is the most stable isomer and also the major isomer in equilibrium. It is also to note that complexes for L = IMes and PPh_3 have the same energetic order and they are also very close in relative energies; and these indicate their high similarity in structures and energies.

Intermediate **B**

It is possible for all six isomers of **A** to form the corresponding complexes **B** from oxidative C–C coupling.

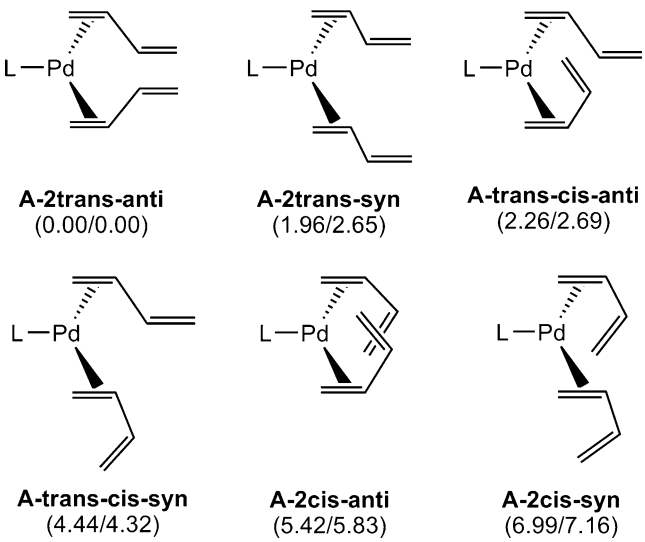

Fig. 1 Conformation and relative free energy (ΔG, kcal mol^{-1}) of LPd (η^2-butadiene)$_2$ complex **A** (L = IMes/PPh_3)

Since **A-2trans-anti** is the most stable isomer, it is interesting to know which isomer will result in the most stable **B**. Hence, we have computed all six conformations along with their corresponding transition states of oxidative C–C coupling. The computed activation free energy ($\Delta G^{\neq}$) and reaction free energy (ΔG) of each C–C oxidative coupling are listed in Table 1.

For the C–C coupling of two *trans*-butadienes (**A-2trans-anti** and **A-2trans-syn**), both reactions have nearly the same activation energies for L = IMes (13.56 and 14.05 kcal mol^{-1}) and L = PPh_3 (15.40 and 15.58 kcal mol^{-1}). Most importantly, these reactions have positive reaction energies (6.89 and 9.29 kcal mol^{-1} for L = IMes; and 11.45 and 12.86 kcal mol^{-1} for L = PPh_3) and are endogonic. Therefore, it is thermodynamically not possible to form the corresponding complex **B-2trans-anti** and **B-2trans-syn** from C–C coupling of two *trans*-butadienes.

For C–C coupling of two *cis*-butadienes (**A-2cis-anti** and **A-2cis-syn**) both reactions have the largest barriers and are nearly thermal neutral for L = IMes and PPh_3. Therefore, these reactions are neither kinetic nor thermodynamic accessible, and the corresponding complex **B-2cis-anti** and **B-2cis-syn** can not be formed from C–C coupling of two *cis*-butadienes.

For the C–C coupling of one *trans*- and one *cis*-butadiene, there are two different cases. The reactions of two butadienes in *anti* orientation (**A-trans-cis-anti**) have high barriers and are slightly exogonic (L = IMes) or endogonic (L = PPh_3). For two butadienes in *syn* orientation (**A-trans-cis-syn**), however, the reaction has the lowest barriers and is most exogonic. Apparently, this reaction path is favorable both kinetically and thermodynamically, and represents the only way for the formation of complex **B-trans-cis-syn**.

Interestingly, the less stable **A-trans-cis-syn**, rather than the most stable **A-2trans-trans**, leads to the formation of the most stable coupling product **B-trans-cis-syn**, the reaction has a pre-equilibrium shift from **A-2trans-anti** to **A-trans-cis-syn**. Since their energy differences (Fig. 1) are much smaller than the activation barriers (Table 1), this equilibrium shift does not control the reaction rate.

Table 1 Computed activation ($\Delta G^{\neq}$, kcal mol^{-1}) and reaction free energy (ΔG, kcal mol^{-1}) for C–C coupling to complex **B** (relative to the respective minimum **A**)

	L = IMes		L = PPh_3	
	$\Delta G^{\neq}$	ΔG	$\Delta G^{\neq}$	ΔG
A-2trans-anti	13.56	6.89	15.40	11.45
A-2trans-syn	14.05	9.29	15.58	12.86
A-trans-cis-anti	17.86	−4.72	20.09	2.07
A-trans-cis-syn	11.15	−6.55	12.13	−2.62
A-2cis-anti	19.86	−0.28	21.36	−1.08
A-2cis-syn	21.66	−1.93	21.23	1.71

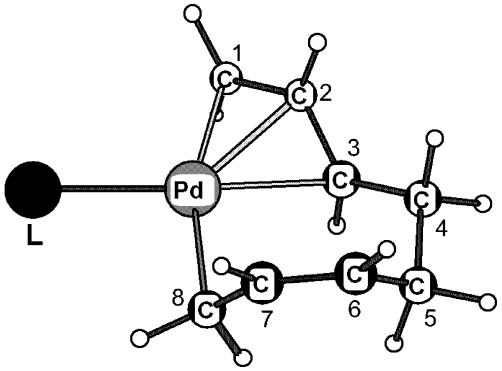

Fig. 2 C8 chain conformation of intermediate B

It is important to note that the most stable intermediate **B** for L = IMes and PPh_3 has the same C8 carbon chain configuration as found experimentally for phosphine ligands [14, 15, 22], *i.e.*, a *trans*-C4 chain in η^3-allylic coordination and a *cis*-C4 chain in η^1-coordination, and the allylic moiety and the *cis*-butene moiety are in *syn* position (Fig. 2). Table 2 shows that that computed structural parameters agree very well with those obtained from X-ray analysis for PMe_3 or PMePh(cyclohexyl) complexes.

Intermediate **C**

Protonation of **B** to **C** is the next step of the reaction. For getting full insight into the mechanism, all isomers of the protonated intermediate **C** have been considered. As given in Table 3, the direct protonation product from the most

Table 2 Computed bond distances for L = IMes and PPh_3, compared with the available X-ray structural data for L = PMe_3 and PMePh (cyclohexyl) of complex B

L	IMes	PPh_3	PMe_3[a]/$PR_1R_2R_3$[b]
Pd-C1	2.208	2.276	2.208/2.210
Pd-C2	2.226	2.226	2.144/2.181
Pd-C3	2.295	2.296	2.267/2.252
Pd-C8	2.139	2.146	2.139/2.127
C1-C2	1.416	1.412	1.385/1.389
C2-C3	1.415	1.420	1.390/1.397
C3-C4	1.510	1.508	1.451/-
C4-C5	1.569	1.571	1.506/1.558
C5-C6	1.504	1.503	1.471/-
C6-C7	1.361	1.361	1.361/1.340
C7-C8	1.476	1.475	1.427/-

a) Ref. [6] b) Ref. [22] (L = PMePh(cyclohexyl)

Table 3 Relative energies (ΔG, kcal mol^{-1}) of complex C

	L = IMes	L = PPh_3
C-2trans-anti + H	−0.95 (15%)	−0.52 (70%)
C-2trans-syn + H	−2.16 (85%)	1.73
C-trans-cis-anti + H	2.20	1.80
C-trans-cis-syn + H	0.00	0.00 (30%)
C-2cis-anti + H	5.15	6.14
C-2cis-syn + H	5.54	7.02
C + H-open	7.245	12.71

stable complex **B** does not represent the most stable complex **C**.

For L = IMes (Table 3), the most stable intermediate **C** is **C-2trans-syn + H** (−2.16 kcal mol^{-1}), followed by **C-2trans-anti + H** (−0.95 kcal/mo), although the corresponding complex **B-2trans-syn** and **B-2trans-anti** cannot be formed from the C–C coupling reactions. The same is also found for L = PPh_3. For example, **C-2trans-anti + H** is most stable (−0.52 kcal mol^{-1}), followed by **C-trans-cis-syn + H** (0.00 kcal mol^{-1}), although the corresponding complex **B-2trans-anti** is not accessible *via* C–C coupling reaction. The other isomers of **C** are much higher in energy (Table 3). The C8 chain conformation and the bond parameters of the two most stable structures of intermediate **C** (L = IMes, PPh_3) are shown in Fig. 3.

Considering the free energy differences, it is to expect that **C-2trans-syn + H** and **C-2trans-anti + H** for L = IMes are in equilibrium with a ratio of 85% to 15%; and **C-2trans-anti + H** and **C-trans-cis-syn + H** for L = PPh_3 are in equilibrium with a ratio of 70% to 30%. These results reveal that this reaction has the second equilibrium shift between protonated intermediates **C** and their rather small energy differences do not affect the reaction rate. In addition to these energetic differences, the equilibrium process has also been computed. Considering that this process effectively involves the decoordination of the alkene part (C7–C8), which can be a significantly activated process, we have tried to localize the transition state of this decoordination, but such transition states could not be located. It is interesting to note that the open-chain complex, **C + H-open**, is only 7.24 and 12.71 kcal mol^{-1} less stable than the corresponding **C-trans-cis-syn + H** for L = IMes and PPh_3, respectively. Such small energy difference shows that the equilibrium process could be not too difficult.

The last step is the nucleophilic attack of MeO^- to produce both *n*- and *iso*-products **D**. Considering the two most stable isomers of **C** in equilibrium, which can form different regioisomers, we have computed all these possibilities (Fig. 4).

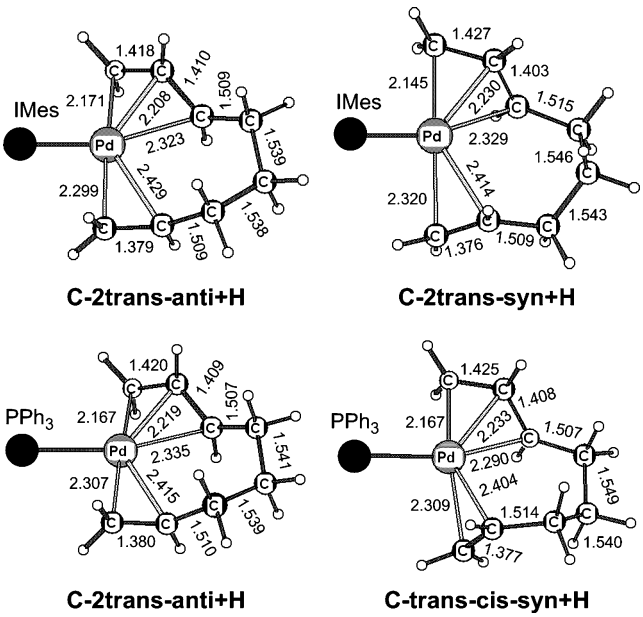

Fig. 3 C8 chain conformation and bond parameters (in Å) of the two most stable isomers of intermediate **C**

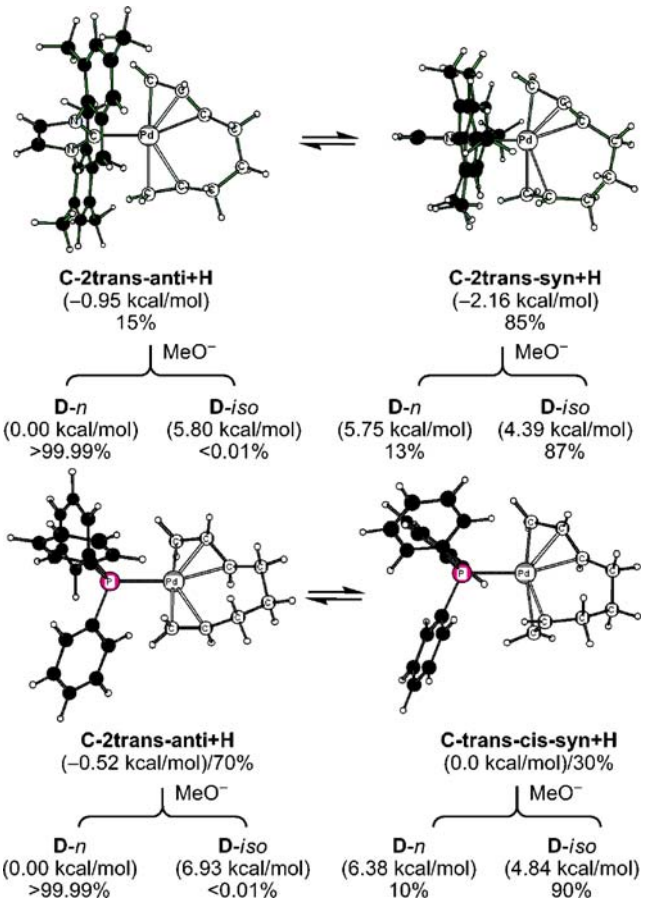

Fig. 4 Reative energies (ΔG) for complexes C and D as well as their equilibrium ratios

The carbene-ligated most stable complex **C-2trans-syn + H** favors **D-*iso*** over **D-*n*** with a ratio of 87% to 13%; while complex **C-2trans-anti + H** favors **D-*n*** quantitatively (>99.99%). Since **D-*n*** from **C-2trans-anti + H** is more stable than that from **C-2trans-syn + H** and **D-*iso*** from both processes, the equilibrium should be shifted from **C-2trans-syn + H** to **C-2trans-anti + H** to result in **D-*n*** as the major product. The regioselectivity of two **D** isomers from each intermediate **C** is thermodynamically controlled; and two **D** isomers are in equilibrium. Since two intermediates **C** also are in equilibrium, the overall regioselectivity is the product of the equilibrium of intermediates **C** and the equilibrium of products **D**. The overall regioselectivity from all equilibriums is over 99%. On the other hand for L = PPh_3, the most stable complex **C-2trans-anti + H** favors **D-*n*** quantitatively (>99.99%); and **C-trans-cis-syn + H** favors **D-*iso*** over **D-*n*** with a ratio of 90% to 10%. Similarly **D-*n*** from **C-2trans-anti + H** is more stable than that from **C-trans-cis-syn + H** and **D-*iso*** from both processes. Thus, the equilibrium will be shifted from **C-trans-cis-syn + H** to **C-2trans-anti + H** to result in **D-*n*** as the major product. Again, the overall regioselectivity from all equilibriums is over 99%.

It is to note that the computed regioselectivity is overestimated as compared to the experimentally determined values (98% for L = IMes, and 97% for L = PPh_3). The experimentally determined regioselectivity for L = PPh_3 of 97.3% gives an up limit of the energy difference of 2.12 kcal mol^{-1} for the **D-*n*** and **D-*iso*** products; and this energy difference is overestimated by 4.81 kcal mol^{-1}. For completing the catalytic cycle in Scheme 2, we have also computed the reaction path B with **E** as the intermediate. It is found that the free energy of the formation of **E** is only −0.75 kcal mol^{-1}; and such small quantity reveals the high ligand to metal ratio for the reaction. The computed energy difference of the **D-*n*** and **D-*iso*** products from **E** is 6.35 kcal mol^{-1} in favor of the **D-*n*** isomer. Taking the overestimated energy of 4.81 kcal mol^{-1} into account, the corrected energy difference for **D-*n*** and **D-*iso*** products from **E** is 1.54 kcal mol^{-1}, and this corresponds to a regioselectivity of about 93.1 %, in very good agreement with the experimentally determined regioselectivity of 93.3–94.1% with the a metal to ligand ratio of 1 to 10.

Conclusions

In summary, B3LYP density functional theory computations have been carried out to investigate the Pd-catalyzed telomerization reaction of 1,3-butadiene and methanol with real-sized IMes and PPh_3 ligands. The computed kinetic and thermodynamic parameters show that the less stable isomer with one *trans*- and one *cis*-1,3-butadiene in *syn* orientation (**A-trans-cis-syn**), rather than the most stable isomer with two *trans*-butadienes (**A-2trans-anti**), leads to the formation of the most stable oxidative C–C coupling intermediate **B**. The conformation and the structural parameters of **B** agree perfectly with the X-ray data for phosphine ligands. Compared to the activation energy, the energy difference of the pre-equilibrated isomers of 1,3-butadiene complex **A** does not control the reaction rate, and the rate-determining step is the respective C–C coupling reaction. The second interesting point to be emphasized is that protonation of the most stable intermediate **B** leads to the two most stable isomers of intermediate **C** in equilibrium, although their precursor intermediate **B** cannot be formed from oxidative C–C coupling reactions. Thus, experimental characterizations into the structures and conformation of intermediate **C** are necessary. The overall regioselectivity in favor of the linear product (**D-*n***) is determined by the stability of the complex of the final product, and therefore it is a thermodynamically controlled process.

Acknowledgments This work was supported by the Deutsche Forschungsgemeinschaft (Leibniz Prize) and the Chinese Academy of Sciences.

References

1. Nielsen DJ, Cavell KJ (2006) In: Nolan SP (ed) N-Heterocyclic Carbenes in Synthesis. Wiley-VCH, Weinheim, pp 73–102
2. *Clement ND, Routaboul L, Grotevendt A, Jackstell R, Beller M (2008) Chem Eur J 14:7408–7420
3. *Behr A, Henze G, Johnen L, Reyer S (2008) J Mol Catal A 287:95–101
4. *Palkovits R, Nieddu I, Gebbink RJMK, Weckhuysen BM (2008) ChemSusChem 1:193–196
5. *Gaudin JC, Millet P (2008) Chem Commun 588–590
6. Jolly PW (1985) Angew Chem Int Ed Engl 24:283–295 and references cited therein
7. Vollmüller F, Klein S, Krause J, Mägerlein W, Beller M (2000) Eur J Inorg Chem 1825–1832
8. Jackstell R, Gomez AM, Frisch AC, Klein H, Selvakumar K, Zapf A, Spannenberg A, Röttger D, Briel O, Karch R, Beller M (2002) Angew Chem Int Ed 41:986–989
9. Jackstell R, Frisch AC, Beller M, Röttger D, Malaun M, Bildstein B (2002) J Mol Catal A 185:105–112
10. Viciu MS, Zinn FK, Stevens ED, Nolan SP (2003) Organometallics 22:3175–3177
11. Grotevendt A, Bartolome M, Nielsen DJ, Spannenberg A, Jackstell R, Cavell KJ, Oro LA, Beller M (2007) Tetrahedron Lett 48:9203–9207
12. Harkal S, Jackstell R, Nierlich F, Ortmann D, Beller M (2005) Org Lett 7:541–544
13. Jackstell R, Grotevendt A, Michalik D, El Firdoussi L, Beller M (2007) J Organomet Chem 692:4737–4714
14. Benn R, Jolly PW, Mynott R, Raspel B, Schenker G, Schick KP, Schroth G (1985) Organomet 4:1945–1953
15. Jolly PW, Mynott R, Raspel B, Schick KP (1986) Organomet 5:473–481

16. Jackstell R, Harkal S, Jiao H, Spannenberg A, Borgmann C, Rötger D, Cavell NF, KJ NSP, Beller M (2004) Chem Eur J 10:3891–3900
17. Frisch MJ, Trucks GW, Schlegel HB, Scuseria GE, Robb MA, Cheeseman JR, Montgomery JA, Vreven T Jr, Kudin KN, Burant JC, Millam JM, Iyengar SS, Tomasi J, Barone V, Mennucci B, Cossi M, Scalmani G, Rega N, Petersson GA, Nakatsuji H, Hada M, Ehara M, Toyota K, Fukuda R, Hasegawa J, Ishida M, Nakajima T, Honda Y, Kitao O, Nakai H, Klene M, Li X, Knox JE, Hratchian HP, Cross JB, Adamo C, Jaramillo J, Gomperts R, Stratmann RE, Yazyev O, Austin AJ, Cammi R, Pomelli C, Ochterski JW, Ayala PY, Morokuma K, Voth GA, Salvador P, Dannenberg JJ, Zakrzewski VG, Dapprich S, Daniela AD, Strain MC, Farkas O, Malick DK, Rabuck AD, Raghavachari K, Foresman JB, Ortiz JV, Cui Q, Baboul AG, Clifford S, Cioslowski J, Stefanov BB, Liu G, Liashenko A, Piskorz P, Komaromi I, Martin RL, Fox DJ, Keith T, Al-Laham MA, Peng CY, Nanayakkara A, Challacombe M, Gill PMW, Jonson B, Chen W, Wong MW, Gonzalez C, Pople JA (2004) Gaussian 03, Revision C.02. Gaussian Inc, Wallingford, CT
18. Hay PJ, Wadt WR (1985) J Chem Phys 82:299–310
19. **Huzinaga S, Anzelm J, Klobukowski M, Radzio-Andzelm E, Sakai Y, Tatewaki H (1984) Gaussian Basis Sets for Molecular Calculations. Elsevier, Amsterdam
20. Foresman JB, Frisch AE (1996) Exploring chemistry with electronic structure methods: A guide to using Gaussian, 2nd edn. Gaussian Inc, Pittsburgh, PA
21. Fukuoka A, Fukagawa S, Hirano M, Koga N, Komiya S (2001) Organomet 20:2065–2075
22. Storzer U, Walter O, Zevaco T, Dinjus E (2005) Organomet 24:514–520 and references cited therein

*There are more than 70 papers about butadiene telomerization since 2000

**For polarization functions